Thermorheological Behavior of Polyethylene: Effects of Microstructure and Long Chain Branching

Paula Wood-Adams* and Stéphane Costeux

Department of Chemical Engineering, McGill University, 3610 University Street, Montreal, Quebec H3A 2B2, Canada

Received September 29, 2000; Revised Manuscript Received June 6, 2001

ABSTRACT: The independent and combined effects of long and short chain branching on the thermorheological behavior of polyethylene are described. The activation energy of linear poly(ethylene−butene) increases with butene content to approximately 33−34 kJ/mol and then levels off for butene contents between 7 and 25 wt %. Long chain branched homo-polyethylene is thermorheologically complex and is most sensitive to temperature at low frequency. A technique for determining the activation energy spectra of thermorheologically complex materials is proposed. Short and long branches in the same system synergistically increase the zero-shear rate activation energy.

Introduction

The effect of molecular structure on the viscoelastic behavior of polyethylene is not yet completely understood primarily because of the lack of well-defined samples covering broad ranges of molecular attributes. Now, however, single site catalysts allow the large-scale polymerization of polyethylenes having narrow, reproducible molecular weight distributions, randomly distributed short chain branches, and low levels of long chain branching. The availability of these metallocene polyethylenes (mPE) makes possible the systematic study of relationships between molecular structure and viscoelastic behavior, aiding in the development of reliable molecular models. We report here on the effect of long and short chain branching on the temperature sensitivity of viscoelastic behavior, which is part of a larger study of the effects of molecular structure on the rheological behavior of polyethylene.[1,2]

Time−Temperature Superposition. For many polymers the temperature dependence of viscoelastic behavior can be described using a time shift factor, a_T, and a modulus shift factor, b_T, as shown in eqs 1 and 2.

$$\eta_0(T) = a_T(T)\, b_T(T)\, \eta_0(T_0) \tag{1}$$

$$G_N^0(T) = b_T(T)\, G_N^0(T_0) \tag{2}$$

In these equations, T_0 is an arbitrary reference temperature. Materials that exhibit this behavior are said to be thermorheologically simple, and the shift factors make possible the superposition of dynamic moduli data obtained at several temperatures. For such materials, over relatively narrow temperature ranges far from the glass transition temperature, the temperature dependence of the time scale shift factor often follows an Arrhenius relation. The activation energy, E_a, can be used as a measure of the temperature sensitivity of rheological material functions such as $\eta(T,\dot{\gamma})$.

$$a_T = \exp\left[\frac{E_a}{R}\left(\frac{1}{T} - \frac{1}{T_0}\right)\right] \tag{3}$$

The modulus shift factor is only weakly dependent on temperature and is therefore often neglected. According to the Rouse model,[3] the temperature dependence of the modulus shift factor is given by eq 4.

$$b_T = \frac{\rho T}{\rho_0 T_0} \tag{4}$$

However, this factor does not superpose data for some polymers,[4] and a more generally applicable shift factor definition is not presently available.

Thermorheological Complexity. In some cases the effect of temperature cannot be described by a single time shift factor, and a different shift factor is required at each time. Long chain branched materials often exhibit such thermorheologically complex behavior. Linear materials also exhibit complex thermorheological behavior when the glassy modulus plays an important role in the relaxation i.e., at very high frequencies. This kind of complexity was studied by Plazek[5] and others.[6] In this work we consider relaxation behavior far from the glassy zone and therefore consider linear, amorphous polymers to be thermorheologically simple.

In the case of thermorheologically complex materials, the concept of a single activation energy is not meaningful, since the temperature sensitivity is time-dependent. For example, we can consider each element of a discrete spectrum to have its own time shift factor, as shown by eqs 5 and 6:

$$G'(\omega,T) = \sum_{i=1}^{N} \frac{G_i(\omega\lambda_{i,T})^2}{1 + (\omega\lambda_{i,T})^2} \tag{5}$$

$$\lambda_{i,T} = \lambda_{i,0} \exp\left[\frac{E_{a,i}}{R}\left(\frac{1}{T} - \frac{1}{T_0}\right)\right] \tag{6}$$

where each relaxation mode has its own activation energy, and we neglect the dependency of the plateau modulus on temperature. For such a material the zero shear viscosity can be described in terms of the temperature-dependent relaxation spectrum as in eq 7.

$$\eta_0(T) = \sum_{i=1}^{N} G_i \lambda_{i,T} \tag{7}$$

10.1021/ma0017034 CCC: $20.00
Published on Web 07/25/2001

The zero shear viscosity can also be written in terms of an apparent zero shear rate activation energy, $\hat{E}_a$, as shown in eq 8:

$$\eta_0(T) = \eta_0(T_0)\exp\left[\frac{\hat{E}_a}{R}\left(\frac{1}{T}-\frac{1}{T_0}\right)\right] \quad (8)$$

By combining eqs 6−8 and making use of a truncated Taylor series expansion of the exponential terms [$\exp(x) \cong 1 + x$], we arrive at eq 9.

$$\frac{\hat{E}_a}{R} \cong \frac{\sum_{i=1}^{N} G_i\lambda_{i,0}\frac{E_{a,i}}{R}}{\sum_{i=1}^{N} G_i\lambda_{i,0}} = \frac{\sum_{i=1}^{N} G_i\lambda_{i,0}\frac{E_{a,i}}{R}}{\eta_0(T_0)} \quad (9)$$

Equation 9 can alternatively be written in terms of the continuous relaxation spectrum $H(\lambda)$:

$$\frac{\hat{E}_a}{R} \cong \frac{\int_0^\infty \lambda_0 \frac{E_a(\lambda_0)}{R} H(\lambda_0)\, \mathrm{d}\ln\lambda_0}{\eta(T_0)} \quad (10)$$

where $E_a(\lambda_0)$ is a continuous activation energy spectrum. It is important to note that the apparent activation energy associated with η_0 is not the activation energy associated with the longest relaxation time but rather a weighted average of the activation energy spectrum. We will return to this issue when we present our experimental results.

Previous Work on Polyethylene. Hydrogenated polybutadiene (HPB) is a an analogue of poly(ethylene−butene) and can be synthesized via anionic polymerization, which affords very precise control over molecular structure. Many studies of the effect of molecular structure of HPB on its rheological behavior have been performed in an effort to better understand the behavior of polyethylene.

Carella et al.[4] studied the effect of short chain branch level on the thermorheological behavior of HPB. They found that temperature sensitivity increased with the level of short chain branching (SCB). For very high levels of SCB (butene content >38 mol %) most of the effect of short chain branching could be explained by the change in glass transition temperature, and the variation of the shift factor with temperature followed the WLF equation.[7] Although none of their materials followed Arrhenius behavior, the deviation from Arrhenius behavior decreased as the degree of SCB decreased.

Carella et al.[4] found that eq 11 with $d = 2.3$ described the temperature dependence of the modulus shift factor, b_T, of high vinyl HPB better than the Rouse temperature dependence described by eq 4.

$$b_T = \frac{G_N^0(T)}{G_N^0(T_0)} = \frac{\rho^d T C_\infty^{2d-3}}{[\rho^d T C_\infty^{2d-3}]_0} \quad (11)$$

In eq 11, C_∞ is the characteristic ratio defined by Flory.[8] The temperature dependence of C_∞ is usually expressed in terms of the temperature coefficient κ.

$$\kappa = \frac{\mathrm{d}\ln C_\infty}{\mathrm{d}T} \quad (12)$$

Assuming a constant thermal expansion coefficient, α, and making use of eqs 11 and 12, we can derive eq 13.

$$b_T = \frac{T}{T_0}\exp[(T - T_0)(-\alpha d + \kappa[2d - 3])] \quad (13)$$

In the case of a large negative temperature coefficient as for polyethylene ($\kappa = -1.05 \times 10^{-3}$ 1/K) eq 13 predicts a negative modulus temperature dependence.

Raju et al.[9] found star-branched hydrogenated polybutadiene to be thermorheologically complex. At high frequencies, the shift factor required for superposition of the loss modulus is approximately equal to the shift factor for linear hydrogenated polybutadiene, while at low frequencies it is higher when $T < T_0$ and lower when $T > T_0$. This can be explained by the greater temperature sensitivity of the long relaxation times due to the LCB. The authors demonstrated that the apparent zero-shear activation energy increased linearly with branch length following eq 14

$$(\hat{E}_a)_B = (E_a)_L + \Lambda\frac{M_a}{M_e} \quad (14)$$

where M_a is the arm molecular weight, M_e is the entanglement molecular weight, and the subscripts B and L indicate branched and linear. It was later shown by Carella et al.[10] that the activation coefficient, Λ, depends on chain microstructure. They found that for 1,2-vinyl content less than about 66 mol % (or equivalently 50 mol % butene in an ethylene−butene copolymer) the activation coefficient is constant at 1.05 kJ/mol. Blends of star and linear HPB exhibit similar behavior, and eq 15 holds for the low-frequency activation energy, where ϕ is the volume fraction star molecules.[11]

$$(\hat{E}_a)_B = (E_a)_L + \Lambda\phi\frac{M_a}{M_e} \quad (15)$$

It is much more difficult to establish reliable rules for the effect of molecular structure on thermorheological behavior of polyethylene because of the difficulty of varying structure in a systematic way. However, it has been found that the activation energies of traditional (Ziegler−Natta) high-density polyethylene (HDPE), low-density polyethylene (LDPE), and linear low-density polyethylene are typically 28, 58, and 33 kJ/mol, respectively.[12,13] Highly branched LDPE exhibits complex thermorheological behavior, and 58 kJ/mol is its apparent zero-shear rate activation energy.[12]

Wasserman and Graessley[14] studied several HDPE resins, some of which exhibited viscosity enhancement characteristic of long chain branching. All the HDPE resins had very similar activation energies, and there was no correlation between E_a and the degree of viscosity enhancement. The authors proposed that these materials were very sparsely branched and that linear chains therefore dominated the thermorheological behavior. We will show that sparsely branched polyethylenes do, in fact, have elevated activation energies.

Malmberg et al.[15] studied the thermorheological behavior of linear and long chain branched mPE. They found that linear homopolymer mPE had an E_a of 26 kJ/mol, which is slightly lower than the accepted value of 28 kJ/mol for traditional HDPE. They also reported much higher apparent zero-shear activation energies,

Table 1. Long Chain Branched MPEs

resin	comonomer	density	M_w DRI[a]	M_w LALLS	M_w/M_n DRI	LCB/10^4C ^{13}C NMR	LCB/10^4C rheology[23]	LCB/10^4C GPC[1]
LDB1	octene	0.908	102 000		2.21		0.12	0.1
LDB2	octene	0.908	84 000		2.21		0.41	0.4
LDB3	octene	0.908	83 000		2.32		0.53	0.6
HDB1	none	0.9592	78 000	77 000	1.98	0.26	0.27	0.3
HDB2	none	0.9583	80 000	82 000	1.93	0.37	0.41	0.3
HDB3	none	0.9575	82 000	86 000	1.99	0.42	0.46	0.4
HDB4	none	0.9565	84 000	96 000	2.14	0.80	0.76	0.8

[a] DRI = differential refractive index detector.

Table 2. Linear Butene Copolymers

resin	M_w DRI	M_w LALLS	M_w/M_n DRI	wt % butene
HDL1	94 000	93 000	2.08	1.4
LDL1	110 000	109 000	2.30	11.4
LDL2	98 000	97 000	2.08	14.83
LDL3	121 000	120 000	2.12	21.2

up to 57 kJ/mol for some materials, which, according to ^{13}C NMR, had levels of LCB below 2 LCB/10^4C.[16] Malmberg et al.[15] concluded the measured degree of branching to be inconsistent with an apparent activation energy essentially equal to that of very highly branched LDPE. The materials with elevated $\tilde{E}_a$ were also thermorheologically complex.[15]

Experimental Section

Materials. The naming convention we have used is as follows: the first two letters refer to either "high density" or "low density", the third letter is L for linear materials and B for branched materials, and the number indicates its place in a series. The long chain branched polymers listed in Table 1, LDB1−3 and HDB1−4, were synthesized using a "constrained geometry" catalyst (Stevens[17,18]) in solution in a continuous, stirred-tank reactor, as described by Lai et al.[19] Soares and Hamielec[20] have explained why this arrangement is optimal for LCB formation. Branching occurs by the insertion of vinyl-terminated polymer chains to active centers during polymerization. These "macromonomers" are formed primarily by β-hydride elimination. Soares and Hamielec have developed kinetic models for the synthesis of both homopolymers[20] and copolymers,[21] and their models indicate that most of the branched molecules in the branched polymers used in the present study contain a single branch. Sample HDL1 (Table 2) was polymerized in a slurry process on a supported, constrained-geometry catalyst system. Samples LDL1−3 (Table 2) are commercial Exact polymers made by Exxon.

These materials comprise three sets that allowed us to study the effect of short and long chain branching on thermorheological behavior. To study independently the effect of short chain branching, four linear ethylene−butene copolymers (Table 2) were used. Two series of long chain branched metallocene polyethylenes were also studied (Table 1). Within each of these series, the materials have approximately the same molecular weight distribution, and comonomer content (in the case of the low-density resins), but different levels of long chain branching. These materials allowed us to study the effect of LCB and the also combined effects of SCB and LCB on thermorheological behavior.

Molecular weight distributions were determined by high-temperature gel permeation chromatography (GPC) using a differential refractive index (DRI) detector. The system consisted of a Waters 150C GPC with three Polymer Laboratories Mixed-B 10 μm columns. Calibration was performed with narrow polystyrene standards. Absolute molecular weights were also determined on a Polymer Laboratories PL210 high-temperature GPC equipped with a Viscotek model 210R viscometer and a Precision Detectors PD2000 light scattering instrument. In all GPC analyses the solvent was 1,2,4 trichlorobenzene, and the stabilizer (butylated hydroxytoluene) level was 180 ppm. Additional experimental details of the molecular structure analysis are given by Wood-Adams et al.[1]

The number of long chain branches per 10^4 carbon atoms was determined using ^{13}C NMR as described by Randall,[22] from solution properties,[1] and by a rheological technique described by Wood-Adams and Dealy.[23]

Rheological Measurements. All linear viscoelastic data were obtained using a Rheometeric Scientific ARES rheometer in parallel plate (25 mm diameter) configuration, with a gap of 1 mm. All experiments were performed under a nitrogen atmosphere, and resin stability under testing conditions was verified. This instrument has a spring torque transducer with a range of 2−2000 gmf·cm, and torques above 5 gmf·cm were deemed to be reliable. Prior to performing frequency sweeps, strain sweeps were performed to establish the linear region at each frequency. For the frequency sweeps, the variable strain technique was used, which entails using the maximum strain still within the linear region for each frequency. Measurements were performed at 130, 150, and 170 °C for low-density mPE and 150, 170, and 190 °C for the high-density series. The accuracy of measured temperatures was confirmed to be ±0.001 °C using a platinum resistance temperature detector. Under normal operating conditions the control system maintains the temperature within ±0.02 °C of the set point. All data are averages of several repeat measurements performed using different samples.

Creep experiments were performed at 150 °C using a Rheometric Dynamic stress rheometer 5000 (SR-5000) in parallel plate configuration (25 mm diameter) with a gap of 1 mm. A nitrogen atmosphere was used to prevent thermal degradation, and stability under testing conditions was verified. Measurements at several stresses were performed to confirm linear behavior. All data are averages of several repeat measurements performed using different samples.

Results and Discussion

Determination of Zero-Shear Viscosity. An important part of this study was the determination of the zero-shear viscosity for the LCB materials. Since these materials have long relaxation times, and all the experiments were carried out in the frequency range from 0.01 to 500 rad/s, the Newtonian plateau at low frequency could not be obtained for all samples. Therefore, η_0 was estimated by fitting a well-behaved viscosity model to the data. For the linear materials (LDL1−3 and HDL1), the Cross equation was used:

$$\eta^*(\omega) = \eta_0/[1 + (\lambda\omega)^n] \tag{16}$$

The value of n was assumed independent of temperature, and the characteristic time, λ, was taken to be proportional to η_0. For the linear samples the values obtained for the zero-shear viscosity from the Cross equation were within 3% of those inferred from the spectrum (and less than 1% for LDL1 and LDL3). In the case of the branched materials (LDB and HDB), unique solutions were not found when fitting eq 16. Instead, a discrete relaxation spectrum was determined using a method described by Kaschta et al.[24] to obtain

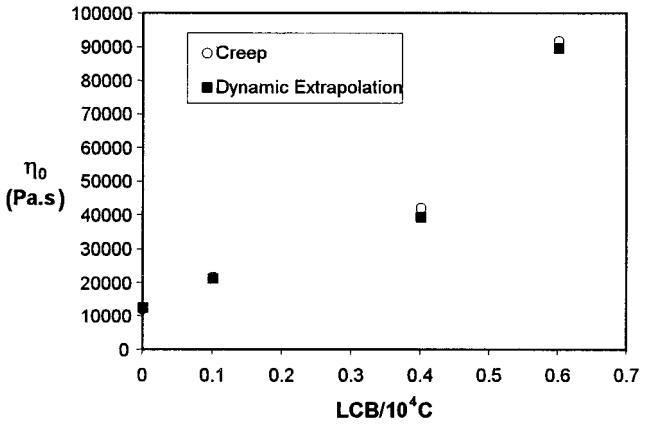

Figure 1. Comparison between extrapolated and measured values of zero-shear viscosity (LDL1, LDB1−3, 150 °C).

Table 3. Temperature Coefficients of Several Polyolefins

polymer	SCB/ backbone C	length of SCB (no. C)	$10^3\kappa$ (1/°C)
polyethylene	0	n.a.	−1.05[26]
polybutene	0.5	2	0.50[26]
poly(*n*-pentene)	0.5	3	0.53[26]
poly (ethylene−butene) [8 mol % butene]	0.08	2	−0.64[a]

[a] Estimated using eq 7 and experimental modulus shift data from Carella et al.[4]

the best fit with 7−10 modes, and a first indication of the zero shear viscosity was given by

$$\eta_0 = \sum_{i=1}^{N} G_i \lambda_i \tag{17}$$

To check the reliability of these estimates, we performed creep studies on LDL1 and LDB1−3 at 150 °C (Figure 1) and found good agreement between the estimated and measured values. As expected, for branched materials the extrapolations using the discrete spectra slightly under predicted the measured zero shear viscosities (maximum difference of 6%). From these results we concluded that the estimated values of η_0 were adequate for our purposes.

Determination of Modulus Shift Factor. One of the goals of this work was to test the applicability to mPE of two models describing the temperature dependence of b_T (eqs 4 and 11). According to the Rouse model, the thermal expansion coefficient, α, is the only material dependent parameter necessary to predict b_T. If we assume that polyethylene melt density is not affected by branching and that α is independent of temperature and equal to 0.000657 1/°C (average value between 130 and 190 °C[25]), then the modulus shift for all polyethylenes is given by eq 18.

$$b_T = \frac{T}{T_0} \exp(-0.000657(T - T_0)) \tag{18}$$

In the model proposed by Carella et al.[4] (eq 11) there are two material-dependent parameters, κ and α, where κ is dependent on the level and length of short chain branches. Reported values for the temperature coefficients for polyethylene, polybutene, and poly(*n*-pentene)[26] are shown in Table 3. We see that κ increases with the number of short branches per backbone carbon and with the length of short branches. Since there were

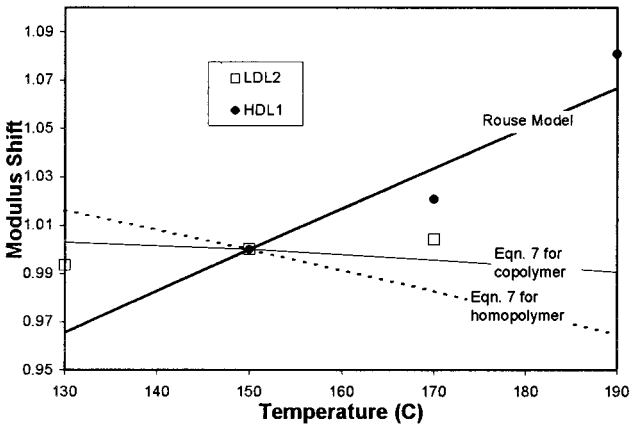

Figure 2. Effect of temperature on modulus shift factor for linear polyethylene.

no published data for poly(ethyelene−butene), we applied eq 7 to the linear viscoelastic data of Carella et al.[4] and estimated that $\kappa \cong -0.64 \times 10^{-3}$ 1/°C for poly(ethylene−butene) with 8 mol % butene. This value seems reasonable as it falls between the values for polyethylene and polybutene. To test the applicability of the two models to mPEs, we then compared numbers calculated using eqs 13 and 18 with our experimental data.

In the absence of a distinct plateau in the storage modulus, the temperature dependence of the maximum value of the loss modulus is often used to determine b_T. However, the materials in this study did not exhibit maxima in their loss moduli within the experimental window, and we calculated b_T from the crossover modulus, G_X, as shown by eq 19.

$$b_T(T) = \frac{G_X(T)}{G_X(T_0)} \tag{19}$$

When data points did not fall exactly on the crossover point, Akima cubic spline interpolation[27] was used to estimate G_X. The long chain branched materials have dynamic moduli curves that are very close together over more than a decade of frequency, leading to high uncertainty in the estimated G_X. For this reason, and because the modulus shift factors estimated in this way for the long chain branched materials did not follow any discernible temperature dependence, we decided to focus our attention on the linear materials. In Figure 2, values of b_T calculated from eqs 18 and 13 are compared with experimental values for HDL1 (homopolymer) and for LDL2 (poly(ethyelene−butene), 8 mol % butene). For HDL1, the data are in better agreement with the Rouse model than with eq 13, which predicts a negative temperature dependence. For LDL2, eq 13 predicts very little change in b_T between 130 and 190 °C. The data also show very little change with temperature. Considering the uncertainty in the estimation of κ, the fit of eq 13 for this material is quite good. We thus conclude that neither the Rouse model nor eq 13 is generally applicable to polyethylene and poly(ethylene−α-olefins).

Establishing Thermorheological Complexity. Careful examination of data is necessary before concluding that a material is thermorheologically simple. For example, in Figure 3 an apparent master curve for the loss modulus of HDB4 is presented. A single frequency shift factor was used for each temperature, and the data appear to superpose well. However, at the low frequency end of the curve the data shifted from

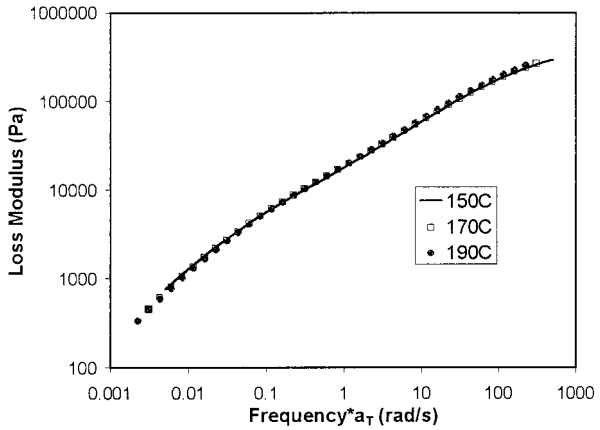

Figure 3. Apparent thermorheological simplicity (HDB4, T_0 = 150 °C, a_T(170 °C) = 0.62, a_T(190 °C) = 0.45).

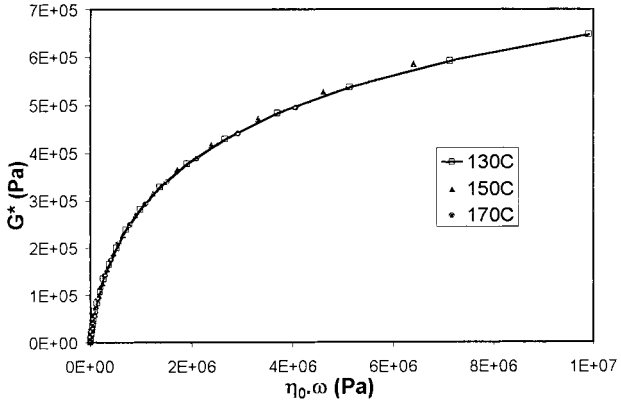

Figure 4. An example of simple behavior (LDL1).

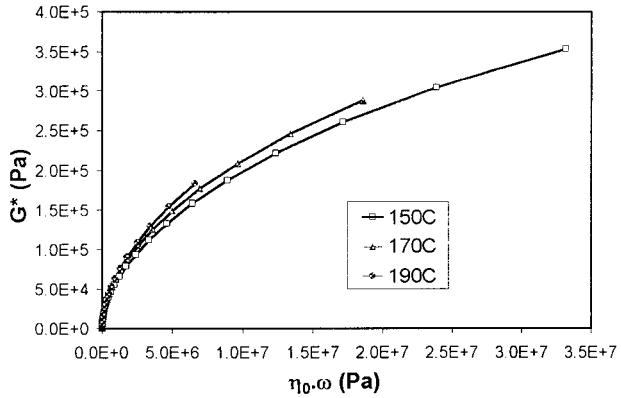

Figure 5. An example of complex behavior (HDB4).

190 °C are slightly below those from 170 °C, which are slightly below those from 150 °C. An inverse trend exists at high frequency but is less noticeable in this plot. This apparent superposition is the result of using an average a_T rather than one based upon the zero shear viscosity. Such average shift factors are the result of attempting to superpose both the storage and loss moduli at all frequencies using a single shift factor.

Plots of the magnitude of the complex modulus vs the product of zero-shear viscosity and frequency are useful for detecting thermorheologically complex behavior. Such plot are temperature independent for simple materials (Figure 4) and temperature dependent (Figure 5) for complex materials. According to this criterion, all of our linear materials are thermorheologically simple and all of our branched materials are thermorheologically complex.

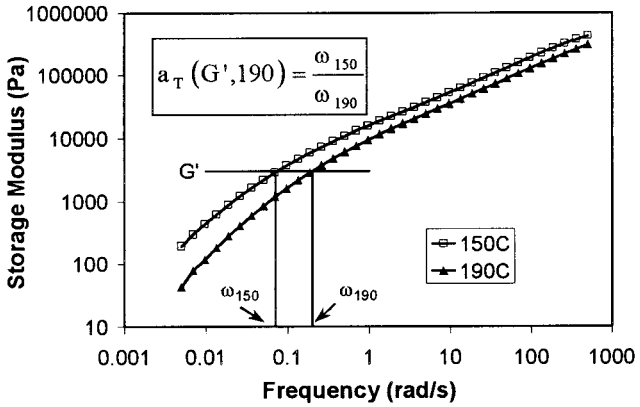

Figure 6. Illustration of modulus-dependent shift factor calculation (HDB4).

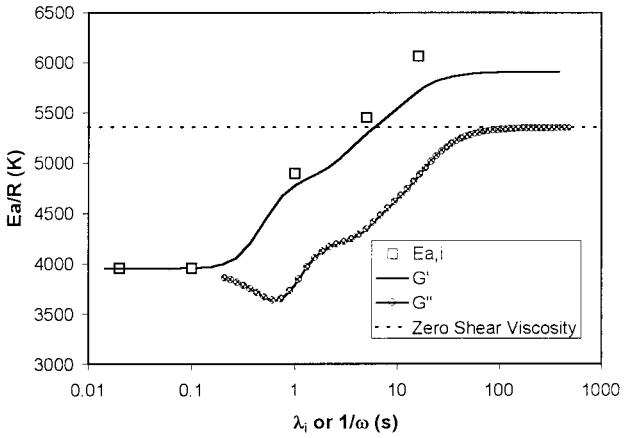

Figure 7. Analysis of simulated material.

Table 4. Simulated Spectrum

G_i (Pa)	$\lambda_{i,0}$ (150 °C) (s)	$E_{a,i}/R$ (K)
53 400	0.02	3950
16 000	0.1	3950
4 000	1	4900
1100	5	5450
430	16	6070

Interpretation of Thermorheologically Complex Data. When complex behavior is exhibited, time−temperature superposition is not possible, but apparent shift factors and apparent activation energies are often calculated to quantify the temperature sensitivity. However, the interpretation of these apparent quantities is not straightforward. To demonstrate this, we consider the artificial material having the discrete relaxation spectrum shown in Table 4. Using this thermorheologically complex spectrum, we generated loss and storage modulus curves at 130, 150, and 170 °C. We then calculated modulus-dependent apparent shift factors, a_T, for $G'(\omega)$ and $G''(\omega)$, choosing 150 °C as the reference temperature. The method for the determination of a_T for $G'(\omega)$ is illustrated in Figure 6 (the calculation of a_T for $G''(\omega)$ is analogous). We then calculated modulus-dependent activation energies from these shift factors. In Figure 7 we compare the inferred activation energies with those assigned to the various relaxation modes. In this figure we plot the true activation energies ($E_{a,i}$) vs the relaxation times at 150 °C ($\lambda_{i,0}$) and the inferred activation energies, $E_a(G')$ and $E_a(G'')$, as functions of the inverse of frequency at 150 °C. The activation energies inferred from the storage modulus are close to the true values, while those

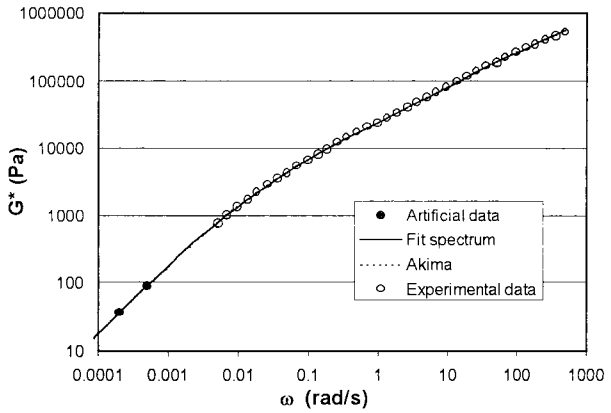

Figure 8. An example of data interpolation (HDB4, 150 °C).

inferred from the loss modulus are much lower and converge to the apparent zero-shear activation energy (eq 8). This can be understood by recalling that the storage modulus is weighted by λ_i^2 (eq 5) while the loss modulus is weighted only by λ_i (eq 20).

$$G''(\omega,T) = \sum_{i=1}^{N} \frac{G_i(\omega\lambda_{i,T})}{1 + (\omega\lambda_{i,T})^2} \qquad (20)$$

These results demonstrate that great care must be taken in quantifying the temperature sensitivity of thermorheologically complex materials. The storage modulus should be used to estimate the activation energy spectrum, $E_a(\lambda)$.

We now apply the preceding analysis to our experimental data. To determine a_T, the dynamic moduli were interpolated between experimental frequencies on a double-logarithmic scale using Akima cubic spline interpolation[27] modified so that outside of the data set the extrapolation was linear. The expected low-frequency power law behavior of the loss modulus could then be obtained by introducing two artificial data points with ordinate $\eta_0\omega$ in the Newtonian plateau. This leads (Figure 8) to low-frequency behavior very close to that obtained from the discrete spectrum, without the inconveniences of the latter (oscillations and poor fitting at high frequencies). Moreover, this ensured that the $a_T(G'')$ determined at low frequencies would be consistent with the values calculated from η_0. For some of the branched samples, the value of η_0 was slightly modified (to a maximum extent of 6%) when a_T was reaching a plateau value in the experimental range that was not consistent with the zero shear viscosity shift factor. The relevance of this alteration was guided by keeping a satisfactory Arrhenius law for η_0. As aforementioned, creep experiments allowed us to check the relevance of the retained zero-shear viscosities.

In the case of the storage modulus, it was not possible improve the quality of the shift by extrapolation, and the shift factors where computed only for values of ω and $a_T\omega$ within the experimental frequency range.

The activation energy spectra, $E_a(1/\omega)$, estimated from the storage modulus for the LDB series and the HDB series are plotted in Figures 9 and 10, respectively. Complex thermorheological behavior arises in polymers that have multiple relaxation regimes with different temperature sensitivities. For the materials studied in this work the complexity is a result of the presence of long chain branches, which have different relaxation

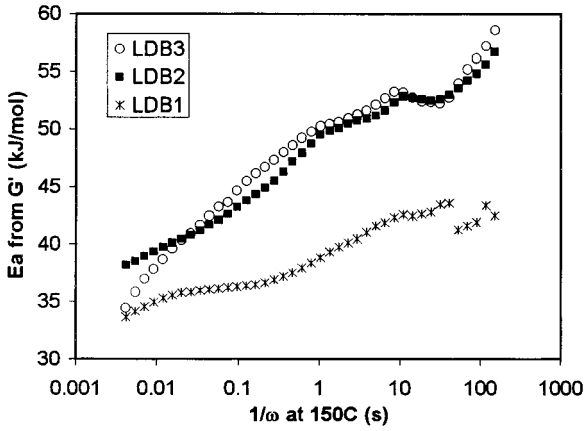

Figure 9. Effect of LCB on time-dependent activation energy (LD series).

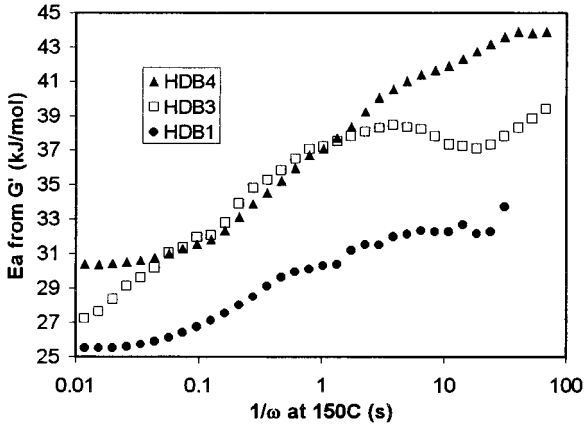

Figure 10. Effect of LCB on time-dependent activation energy (HD series).

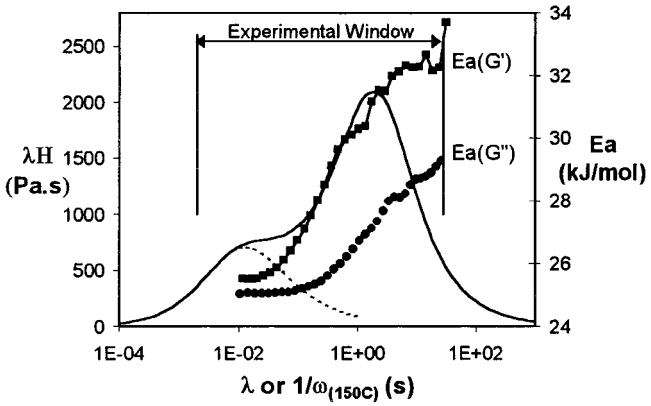

Figure 11. Continuous relaxation spectrum and time-dependent activation energy. HDB1 at 150 °C. Dashed line represents approximate contribution of the linear molecules to the overall relaxation spectrum. Points are (interpolated) experimental activation energy data plotted against $1/\omega_{(150C)}$.

mechanisms than linear chains.[28] To illustrate this point, we examine the continuous relaxation spectrum for HDB1 at 150 °C (Figure 11), which was calculated from the dynamic modulus using the technique developed by Honerkamp and Weese.[29] As demonstrated by Wood-Adams et al.,[30] the short-time peak in the spectrum is due to the reptation of the linear chains. The broad, long-time peak is a cumulative effect of the relaxations of molecules having various branching structures. The dashed curve represents the approxi-

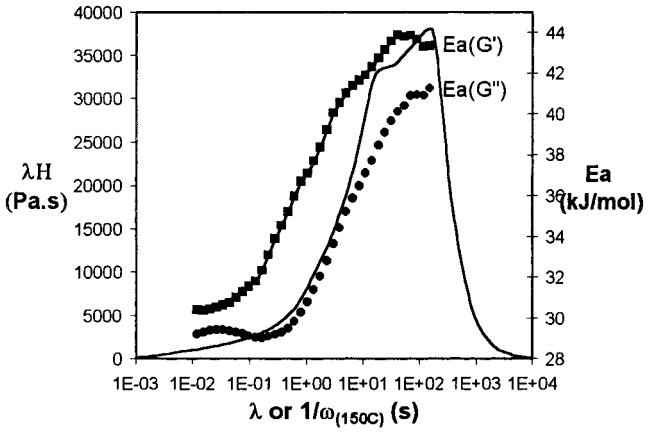

Figure 12. Continuous relaxation spectrum and time-dependent activation energy. HDB4 at 150 °C. Points are (interpolated) experimental activation energy data plotted against $1/\omega_{(150C)}$.

mate contribution of the reptation of the linear chains to the system's behavior while the branched molecules are also relaxing. For comparison, the two activation energy functions determined from $G'(\omega)$ and from $G''(\omega)$ are plotted against the inverse of the frequency at 150 °C on the same figure. At the shortest times, the stress relaxation behavior of HDB1 is dominated by the reptation of the linear chains. At these times $E_a(G')$ and $E_a(G'')$ converge to approximately the same activation energy as a purely linear system of equivalent microstructure. At longer times the stress relaxation behavior is dominated by the branched molecules, which are more sensitive to temperature. As expected, $E_a(G')$ and $E_a(G'')$ diverge sharply when thermorheological complexity is present. At intermediate times both activation energies are approximately linearly related to the logarithm of time in accord with the molecular model of Levine and Milner.[31] This model provides a qualitative understanding of the thermorheology of monodisperse stars of HPB by incorporating an energy barrier for the hairpin turns that occur during arm retraction. Arm retraction is the only mechanism available for the relaxation of free arms (molecular segments with one free end and one branch point).

All of the long chain branched materials exhibited behavior similar to HDB1. For comparison, the results for HDB4 are presented in Figure 12. Since HDB4 has a higher degree of long chain branching, the change in the activation energy from short time to long time is much larger.

While the model of Levine and Milner offers some enlightenment on the behavior of monodisperse stars, it does not allow for the exact deconvolution of the temperature sensitivities of the polydisperse systems that we are dealing with. As a first approximation, we fitted the relaxation spectrum of HDB1 at 150 °C as the sum of two Gaussian functions (Figure 13) centered at λ_1 and λ_2 as shown in eq 21.

$$H_0(\lambda) = H_0^{(1)}(\lambda) + H_0^{(2)}(\lambda)$$

$$\text{with } H_0^{(i)}(\lambda) = G_i(2\pi\sigma_i^2)^{-1/2} \exp\left(\frac{-[\log(\lambda/\lambda_i)]^2}{2\sigma_i^2}\right) \quad (21)$$

The parameters for eq 21 are given in Table 5. From Figure 13b we see that the two-mode fit is not successful at long times.

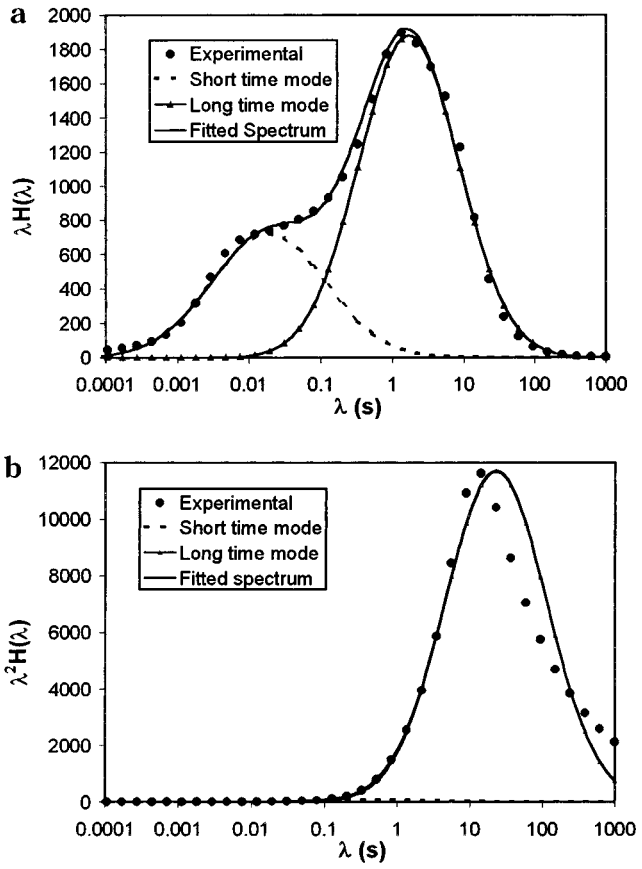

Figure 13. Two mode approximation of relaxation spectrum of HDB1. In (a) the first moment of the spectrum, $\lambda H(\lambda)$, is plotted, and in (b) the second moment, $\lambda^2 H(\lambda)$, is plotted.

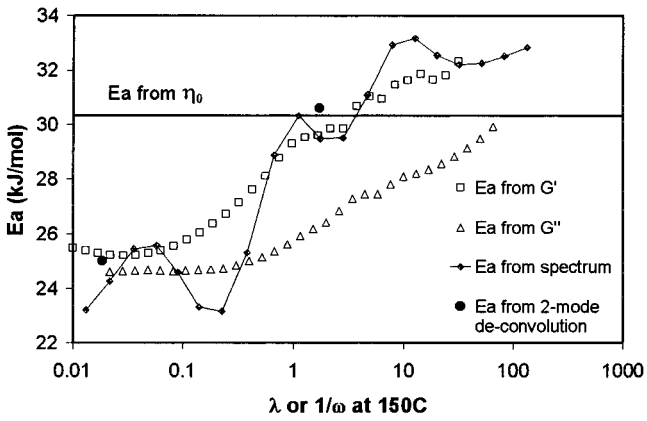

Figure 14. Comparison of activation energy spectra inferred via different techniques.

Table 5. Approximate Deconvolution of Temperature Sensitivity of HDB1

λ_i (150 °C)	G_i (150 °C)	σ_i (150 °C)	a_T (190 °C)	E_a (kJ/mol)
0.0186	1450	0.8	0.540	25.0
1.698	3330	0.7	0.472	30.6

Next we assumed that each mode has a single activation energy and fitted eq 22 to the spectra at 190 °C, resulting in the shift factors shown in Table 5.

$$H_T(\lambda) = H_0^{(1)}(\lambda/\alpha_T^{(1)}) + H_0^{(2)}(\lambda/\alpha_T^{(2)}) \quad (22)$$

In Figure 14 the two discrete activation energies that result from the previous approximate analysis are compared with those estimated from the loss and

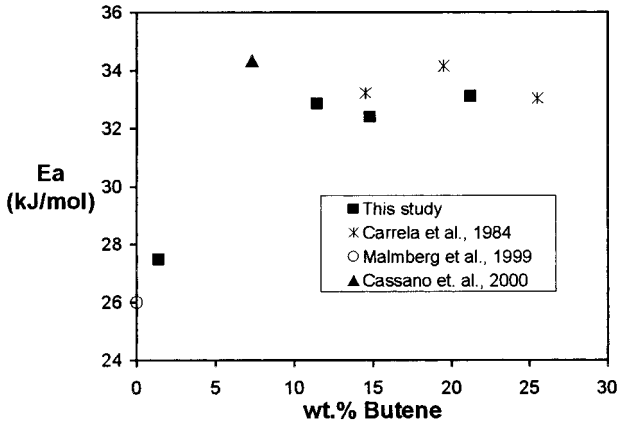

Figure 15. Effect of short chain branching on the flow activation energy of linear poly(ethylene−butene). Data from Carrela et al.[4] and Cassano et al.[32] are for hydrogenated polybutadiene; data from Malmberg et al.[15] are for linear homo-polyethylene mPE.

storage moduli and with a set inferred by attempting to shift the real spectra (rather than assuming only two activation energies). The most direct way of determining the activation energies for the various relaxation mechanisms is from the spectra, but this is very sensitive to small inaccuracies in the spectra and causes oscillations in the results. The two-mode approximation does not give quantitative agreement because in reality the activation energy varies continuously with relaxation time, and the relaxation behavior cannot be accurately modeled with two Gaussian curves (Figure 13b). From the results in Figure 14 we conclude that the activation energies estimated from the storage modulus give the most accurate estimate of the activation energy spectrum. Future work is planned to develop more rigorous techniques for decoupling the various temperature dependencies in long chain branched mPE.

Effect of Branching on the Apparent Zero-Shear Activation Energy. The apparent activation energy based on the zero-shear viscosity is significantly affected by the presence of long chain branching. As discussed earlier, this apparent activation energy does not correspond to the temperature sensitivity of the longest relaxation time and instead is a weighted average of the activation energy spectrum. When comparing various thermorheologically complex materials, it is convenient to use the zero-shear apparent activation energy, as it is theoretically experiment independent.

Arrhenius activation energies based on η_0 were calculated by fitting the linearized form of eq 3 using least-squares regression. The effect of short chain branching on the flow activation energy of linear polyethylene is shown in Figure 15. The combined effects of long and short chain branching are shown in Figure 16, and the activation energy values are tabulated in Table 6.

The activation energy of HDL1 is 27.5 kJ/mol, which is consistent with reported values for HDPE. The LDL materials, which have much higher levels of comonomer than HDL1, have activation energies consistent with reported values for traditional LLDPE, and there is no correlation between butene content and E_a. On the basis of a comparison of these results with selected data from the literature[4,15,32] (Figure 15), it appears that E_a initially increases with butene content and then levels off at about 33−34 kJ/mol for butene contents higher than 7 wt %. At 150 °C the LDL materials follow the same zero-shear viscosity vs M_w behavior that was

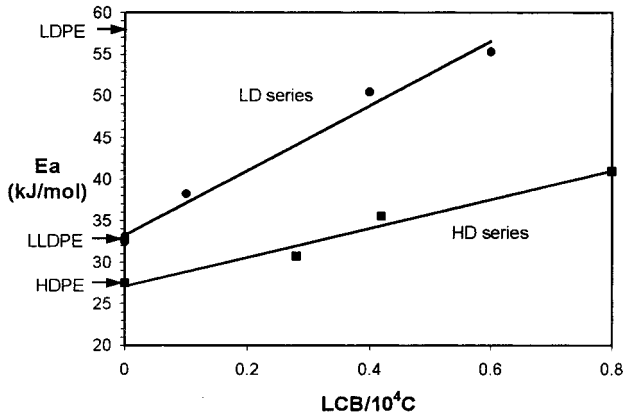

Figure 16. Synergistic effect of long and short chain branching on zero-shear activation energy of polyethylene (lines are to aid the eye only).

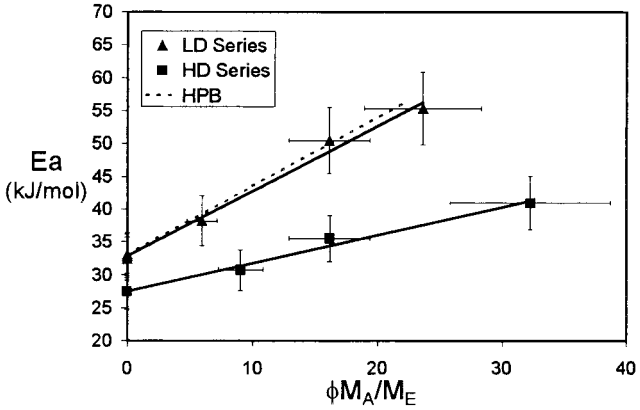

Figure 17. Relationship between branching level and flow activation energy for polyethylene (HD series), poly(ethylene−butene) with 4 mol % butene from Carella et al.,[10] and poly(ethylene−octene) with 4 mol % octene (LD series).

Table 6. Zero Shear Activation Energies

resin	η_0 (150 °C) (Pa·s)	$\hat{E}_a$ (kJ/mol)	resin	η_0 (150 °C) (Pa·s)	$\hat{E}_a$ (kJ/mol)
LDL1	12 700	32.9	LDB3	90 000	55.3
LDL2	10 600	32.4	HDL1	6 000	27.5
LDL3	22 600	33.1	HDB1	10 900	30.7
LDB1	21 500	38.2	HDB3	57 800	35.5
LDB2	39 700	50.4	HDB4	177 800	40.9

found for homo-polyethylene[1] (η_0[Pa·s] = 6.8 × 10^{-15} $M_w^{3.6}$), but this is not the case at other temperatures. For linear polyethylene the entire effect of SCB on LVE behavior is contained in the zero-shear viscosity, and SCB level independent plots can be obtained in the same manner as M_W independent plots.[1]

As expected, we find that long chain branching increases the zero shear temperature sensitivity of polyethylene (Figure 16). Moreover, there is a synergistic effect when long and short branches are both present, resulting in a heightened dependence of $\hat{E}_a$ on degree of LCB when SCB is also present. It appears to be the combination of long and short branches that gives mPE such high flow activation energies (on a par with LDPE) at relatively low levels of LCB. And it is likely that it is the combination of long and short branches that gives high-pressure LDPE its high activation energy (ca. 58 kJ/mol). Questions remain about the effect of comonomer type and content on the LCB dependence of the apparent, zero-shear activation energy, and future work is planned in this area.

These results bring into question some of the rheological techniques that have been developed to determine the level of LCB, as most of these techniques do not properly account for the effect of the short branches. A technique recently developed by Shroff and Mavridis[33] failed to rank correctly our branched materials in terms of degree of LCB, presumably because of these factors.[23] A long chain branching index defined by Vega et al.,[34] which makes use of the difference between the $\hat{E}_a$ of a long chain branched material and that of a linear material with the same comonomer content, also fails, because it does not account for the increased dependence of E_a on LCB in the presence of SCB.

Since long chain branched mPE can be considered to be a mixture of linear, T-shaped and H-shaped molecules with very few more highly branched molecules,[35] and the relationship between $\hat{E}_a$ and degree of LCB is linear, we fitted a slightly modified version of eq 15. We first define the fraction of molecules that are branched, ϕ, as in eq 23

$$\phi \equiv \frac{M_w}{M_1 \times 10^4}\left(\frac{\text{LCB}}{10^4\text{C}}\right) \tag{23}$$

where the molecular weight of the repeat unit, M_1, is 14 g/mol. The weight-average arm length is then assumed to be approximately equal to the overall weight-average molecular weight. For M_e we use 1250 g/mol as estimated by Raju et al.[9] Finally, eq 15 becomes eq 24.

$$(\hat{E}_a)_B = (E_a)_L + \Lambda \frac{{M_w}^2}{2.1 \times 10^8}\left[\frac{\text{LCB}}{10^4\text{C}}\right] \tag{24}$$

Graessley and Raju[11] found this equation to be valid for blends of linear and star HPB, which are approximate analogues of branched mPE. Using least-squares regression, the activation coefficient was determined to be 1.0 kJ/mol for the LD octene copolymers and 0.4 kJ/mol for the HD homopolymers. The LD and HD materials are described by eqs 25 and 26, respectively.

$$(\hat{E}_a)_B = 32.8 + 4.721 \times 10^{-9}{M_w}^2\left[\frac{\text{LCB}}{10^4\text{C}}\right], \quad r^2 = 0.992 \tag{25}$$

$$(\hat{E}_a)_B = 27.5 + 2.028 \times 10^{-9}{M_w}^2\left[\frac{\text{LCB}}{10^4\text{C}}\right], \quad r^2 = 0.983 \tag{26}$$

It is expected that eq 25 would be applicable to all poly(ethylene−octene) resins that contain 4 mol % octene and were synthesized using constrained geometry catalysts. Equation 26 should be applicable to all homopolyethylenes synthesized using the same catalysts. Equations 25 and 26 are compared to the fit of Carella et al.[10] for HPB (analogous to poly(ethylene−butene)) in Figure 17. The error bars represent 20% uncertainty in ϕM_A and 10% uncertainty in E_a. The activation coefficient for the LD (1.0 kJ/mol) series is approximately the same as that for HPB (1.05 kJ/mol). It is important to note that eqs 23 and 24 cannot be used to quantify LCB, since the activation coefficient is highly dependent on comonomer content and probably also dependent on the structure of the long chain branches.

At this point it is useful to reexamine the data of Malmberg et al.[15] and Wasserman and Graessley[14] in light of our results. Malmberg et al.[15] found what appeared to be unusually high activation energies for long chain branched mPE. However, eq 25 indicates that a homo-polyethylene with $M_w = 110\,000$, and 1.1 LCB/10^4C would have an activation energy of 57 kJ/mol. This means that their measured level of LCB (<2 LCB/10^4C) is not inconsistent with activation energies approaching that of LDPE. Wasserman and Graessley[14] found that low levels of long chain branching did not affect the activation energy of HDPE, which is in contradiction to our results. It seems that these authors may have calculated average shift factors that fitted the entire curves rather than those based on the zero-shear viscosity shift factors. This would result in an average activation energy smaller than the zero-shear activation energy for a long chain branched material.

Conclusions

Long chain branched mPEs are thermorheologically complex, and the low-frequency viscoelastic properties are more sensitive to temperature than the high-frequency properties. The storage modulus provides a good estimate of the activation energy spectrum. The relationship between time and temperature for metallocene polyethylene appears to follow the molecular model of Levine and Milner[31] for stars. The zero-shear activation energy increases with degree of LCB, and the combination of short and long branches has a synergistic effect on this property.

Acknowledgment. Partial financial support for this work as well as all the polymers used and all GPC and NMR data were provided by The Dow Chemical Co. Financial support was also provided by the Natural Sciences and Engineering Research Council of Canada. Linear viscoelastic data were collected by M. Watson and S. Kim. The authors would like to thank Dr. G. McKenna for providing useful comments.

References and Notes

(1) Wood-Adams, P. M.; Dealy, J. M.; deGroot, A. W.; Redwine, O. D. *Macromolecules* **2000**, *33*, 7489−7499.
(2) Wood-Adams, P. M. *J. Rheol.* **2000**, *45*, 203−210.
(3) Rouse, P. E., Jr. *J. Chem. Phys.* **1953**, *21*, 1272.
(4) Carella, J. M.; Graessley, W. W.; Fetters, L. J. *Macromolecules* **1984**, *17*, 2775−2786.
(5) Plazek, D. J. *J. Chem. Phys.* **1965**, *69*, 3480.
(6) Zorn, R.; McKenna, G. B.; Willner, L.; Richter, D. *Macromolecules* **1995**, *28*, 8552−8562.
(7) Ferry, J. D. In *Viscoelastic Properties of Polymers*, 3rd ed.; Wiley: New York, 1980; p 274.
(8) Flory, P. J. *Statistical Mechanics of Chain Molecules*; Carl Hanser Verlag: Munich, 1989.
(9) Raju, V. R.; Rachapudy, H.; Graessley, W. W. *J. Polym. Sci., Polym. Phys. Ed.* **1979**, *17*, 1223−1235.
(10) Carella, J. M.; Gotro, J. T.; Graessley, W. W. *Macromolecules* **1986**, *19*, 659−667.
(11) Graessley, W. W.; Raju, V. R. *J. Polym. Sci., Polym. Symp.* **1984**, *71*, 77−93.
(12) Laun, H. M. *Prog. Colloid Polym. Sci.* **1987**, *75*, 111−139.
(13) Gabriel, C.; Kaschta, J.; Münstedt, H. *Rheol. Acta* **1998**, *37*, 7−20.
(14) Wasserman, S. H.; Graessley, W. W. *Polym. Eng. Sci.* **1996**, *36*, 852−861.
(15) Malmberg, A.; Liimatta, J.; Lehtinen, A.; Löfgren, B. *Macromolecules* **1999**, *32*, 6687−6696.
(16) Malmberg, A.; Kokko, E.; Lehmus, P.; Löfgren, B.; Seppälä, J. V. *Macromolecules* **1998**, *31*, 8448−8454.
(17) Stevens, J. *Stud. Surf. Sci. Catal.* **1994**, *89*, 277−284.
(18) Stevens, J. *Stud. Surf. Sci. Catal.* **1996**, *101*, 11−20.
(19) Lai, S. Y.; Wilson, J. R.; Knight, G. W.; Stevens, J. C. U.S. Patent 5,272,236, 1993.

(20) Soares, J. B. P.; Hamielec, A. E. *Macromol. Theory Simul.* **1996**, *5*, 547−572.
(21) Soares, J. B. P.; Hamielec, A. E. *Macromol. Theory Simul.* **1997**, *6*, 591−596.
(22) Randall, J. C. *J. Macromol. Sci., Rev. Macromol. Chem. Phys.* **1989**, *C29* (2&3), 201−317.
(23) Wood-Adams, P. M.; Dealy, J. M. *Macromolecules* **2000**, *33*, 7481−7488.
(24) Kaschta, J.; Schwarzl, F. R. *Rheol. Acta* **1994**, *33*, 517−529.
(25) Mark, J. E. *Polymer Data Handbook*, Oxford University Press: New York, 1999; p 495.
(26) Mark, J. E. *Rubber Chem. Technol.* **1973**, 593−619.
(27) Akima, H. *J. Association Comput. Machinery* **1970**, *17*, 589−602.
(28) MacLeish, T. In *Chemical Topology: Introduction and Fundamentals*; Bonchev, D., Rouvray, D. H., Eds.; Gordon and Breach Science Publishers: Langhorne, PA, 1999; Chapter 6.
(29) Honerkamp, J.; Weese, J. *Rheol. Acta* **1993**, *32*, 65−73.
(30) Wood-Adams, P. M.; Dealy, J. M.; Costeux, S. *Polym. Mater. Sci. Eng.*, in press.
(31) Levine, A. J.; Milner, S. T. *Macromolecules* **1998**, *31*, 8623−8637.
(32) Cassano, G. A.; Vallés, E. M.; Quinzani, L. M. *J. Rheol.* **2000**, *44*, 47−63.
(33) Shroff, R. N.; Mavridis, H. *Macromolecules* **1999**, *32*, 8454−8464.
(34) Vega, J. F.; Santamaria, A.; Munoz-Escalona, A.; Lafuente, P. *Macromolecules* **1998**, *31*, 3639−3647.
(35) Soares, J.; Hamielec, A. In *Metallocene-Catalyzed Polymers: Materials, Properties, Processing and Markets*; Benedikt, G. M., Goodall, B., Eds.; Plastics Design Library: New York, 1998; pp 103−112.

MA0017034